Interplanetary Shock-Auroras: Multiple Observations

X.-Y. Zhou and B.T. Tsurutani
Jet Propulsion Laboratory
California Institute of Technology, Pasadena, California

C.W. Carlson
Space Sciences Laboratory
University of California, Berkeley, California

R.J. Strangeway
Institute of Geophysics and Planetary Physics
University of California, Los Angeles, California

P.C. Anderson
Space Science Application Laboratory
The Aerospace Corporation, Los Angeles, California

D.G. Sibeck
Applied Physics Laboratory
Johns Hopkins University, Laurel, Maryland

Submitted to Advances in Space Research (ASR), 5/--/2001

Abstract

Interplanetary shocks can trigger intense dayside auroral brightenings and very fast anti-sunward auroral expansions. These auroral phenomena are called "shock-auroras". In this paper, a shock-aurora event that occurred on November 22, 1997 is studied using coordinated observations from the solar wind to the ground. The observations include the data of WIND, POLAR UVI, FAST, DMSP and the ground IMAGE magnetometer chain. WIND detected an interplanetary shock in the upstream solar wind at ~ 0912 UT. POLAR UVI recorded an intense shock-aurora at ~ 0951 UT. FAST and DMSP observations show that above the dawnside auroral oval, downward electron and ion fluxes increased significantly after the interplanetary shock arrival at the dayside magnetopause. Magnetic vortices caused by the shock compression were observed by the IMAGE chain near local noon. The potential drop caused by magnetic shearing is calculated to be ~ 2 kV, a value consistent with the FAST and DMSP energetic electron observations.

1. Introduction

Dayside auroras, as evidence of dynamic processes in the dayside geospace, occur mainly at auroral oval latitudes and can be identified in ultraviolet wavelengths. Substantial dayside auroras have been detected by Viking and POLAR UVI when interplanetary shocks/pressure pulses impinge on the magnetopause (Craven et al., 1986; Arballo et al., 1998; Sitar et al., 1998; Spann et al., 1998; Sibeck et al., 1999; Zhou and Tsurutani, 1999). These "shock-auroras" first brighten near local noon in the auroral zone and then propagate along the auroral oval anti-sunward towards both dawn and dusk (Zhou and Tsurutani, 1999). The auroral propagation speeds in the ionosphere are ~6 to 11 km/s (Tsurutani et al., 2001a), which is much faster than the typical auroral speeds of < 1 km/s (Murphree, 1990). Even with such unusually high speeds and with an opposite sense of propagation from that of typical dawn aurora, these shock-auroras have not been observed from the ground!

Shock-auroras have been explained as particle precipitation caused by a lowering of the mirror points of trapped particles to altitudes below 100 km due to the compression of the magnetosphere (Spann et al., 1998). Further studies by Zhou and Tsurutani (1999), and Tsurutani et al. (2001a; 2001b) have suggested different mechanisms: the loss cone instability, wave-particle interaction, viscous interaction and magnetic field shearing. Their results implied that shock-auroras can manifest in the forms of both diffuse and discrete auroras. Magnetic vortices were found associated with pressure pulse-auroras (Sibeck et al., 1999). Double vortices form at the front edge, where the magnetopause is compressed by interplanetary shocks/pressure pulses which may in turn generate field-aligned currents. This has been suggested as another mechanism for the shock/pressure pulse-auroras (Southwood and Kivelson, 1990; Sitar et al., 1998; Sibeck, 1990 and Sibeck et al.,1999).

In this paper, we present multi-spacecraft observations for a shock-aurora event that occurred on November 22, 1997 to show the shock-aurora related signatures at different altitudes in the magnetosphere. The WIND spacecraft was used to identify and characterize the interplanetary shock, POLAR UVI was used to identify the onset of the shock-aurora brightening and the subsequent auroral expansion. The auroral zone phenomenon is obtained through FAST particle, magnetic field and plasma wave data at ~ 4000 km altitude, DMSP energetic particle data at lower altitudes (~ 840 km), and the ground IMAGE magnetometer chain for geomagnetic variations.

2. Observations for the November 22, 1997 Event.

During this event, WIND was in the upstream solar wind (181, -5, 32 R_e) (in GSM coordinates), POLAR was at (-4.0, 3.1, 4.0 R_e). The FAST satellite was near apogee above the dawnside southern auroral zone when the shock arrived at the magnetopause. DMSP was below the FAST satellite. The IMAGE magnetometer chain was at ~ 12 magnetic local time (MLT).

2.1 WIND and POLAR observations

Figure 1(A) is an interplanetary shock event detected by WIND at ~ 0912 UT, November 22, 1997. At the shock, the interplanetary magnetic field (IMF) magnitude, the solar wind thermal velocity, the plasma density and the solar wind velocity increased (the dashed line) simultaneously. The solar wind ram pressure ($P_{ram} = \rho V^2$) increased from ~ 3 to 13 nPa. The

IMF B_z was near zero about an hour preceding the shock. The calculated shock arrival time at the magnetopause using the shock speed is ~ 0948:45 UT.

Figure 1(B) is the shock-aurora observed by POLAR UVI. The UVI instrument has been described by Torr et al. (1995). The time sequence is from top to bottom. The image cadence is ~ 3 min for this event. Panels (a) and (b) are two images just before the shock arrival, giving a comparison for relative auroral activity. After the shock arrival, at 0951:21 UT (panel c), significant dayside auroral brightening occurred, and the most intense area was near local noon. In panel (d), the dawn flank auroral zone became brighter and wider in the latitudinal direction, showing the shock-aurora expansion anti-sunward along the oval. Although the auroral oval is not completely shown by the images, the shock-aurora brightening onset and the rapid propagation are still clear.

2.2 FAST observations

Interplanetary shocks have very large spatial scales in the directions perpendicular to the shock normal. The typical scales are significant fractions of an AU. Thus, when shocks compress and squeeze the magnetosphere, both northern and southern hemispheres will be affected. Therefore, we assume that the shock-aurora is a conjugated phenomenon at great extent and the particle acceleration and precipitation processes are the same at both hemispheres.

Figure 2 shows FAST observations above the southern auroral zone prior to (panel set a) and after (panel set b) the shock arrival when FAST was near apogee. Both orbits were within the dawn sector from 06 to 09 MLT and across the oval latitudinally from ~ 65° to 83°. Comparing panels (a) and (b), it is shown that this shock causes significant enhancement of wave activity, field-aligned currents, downward electron flux, and isotropic pitch angle scattering at the FAST altitude. Broadband wave activity increased significantly after shock arrival (not shown, to save space).

At ~0956 UT, FAST was at -77.7° magnetic latitude (MLAT) and 08 MLT. FAST detected the downward electron energy flux to be ~ 9.5 eV/cm^2 s sr eV, and the electron energy was ~ 1 keV as shown in the 4th and 5th panels of Figure 2 (b).

2.3 DMSP observations

Figure 3 shows DMSP particle observations after the shock arrival at attitudes beneath FAST. The time is 10 min later than the FAST interval crossing. At 1006 UT, DMSP was at -68.3° MLAT and 06 MLT. The top panel shows that the electron energy flux reached 4.0 ergs/cm^2 s sr at ~ 1006 UT, while ion energy flux reached at ~ 0.1 ergs/cm^2 s sr. The energy of the precipitated electrons was mainly at ~ 5 keV with particle flux higher than 2×10^5 keV/cm^2 s sr eV. The energy of ions was between 0.1 - 1.0 keV with lower particle flux at ~ 3×10^4 keV/cm^2 s sr eV.

2.4 Ground-based magnetometer observations

Ground-based IMAGE magnetometer locations and observations are shown in Figure 4. A map of the IMAGE magnetometer network in geographic coordinates (which is very close to the geomagnetic coordinates in latitude) is shown in panel (a). Collectively, the stations cover ~ 20° in latitude (from 60° to 80°) and ~ 25° in longitude. When the interplanetary shock arrived at the magnetopause, this chain was at ~ 12 MLT.

Figure 4 (b) is a stack plot of the X-components for this event. A sudden magnetic field change occurred at ~ 0949 UT (the vertical line). It is noted that the magnetic field variations detected by higher latitude stations (higher than ~ 75°) were very different from that on mainland Scandinavia, with latitudes lower than ~ 70°. At higher latitude stations, from BJN and above, the X-component increased and then decayed after ~ 20 min. The higher the station latitude, the lesser was the enhancement. But at the stations on the mainland of Scandinavia, the X-component decreased first, then increased within 10 min and decreased again to become a bipolar structure. This bipolar disturbance had a typical magnetic vortex signature (a bipolar signature with a period of about 10 min and an amplitude of typically 100 nT as described by Lühr and Blawert, 1994). The observed amplitude of the bipolar disturbance was reduced toward lower latitudes.

3. Discussion

Adiabatic compression, as one of the shock-aurora mechanisms, has been discussed by Zhou and Tsurutani (1999) and Tsurutani et al. (2001a, 2001b). In this mechanism, electron (and proton) loss-cone instabilities will result, leading to plasma wave growth and particle losses into the auroral ionosphere due to pitch angle diffusion. Intensification of ELF/VLF waves is expected to increase by this instability. In the Nov 22, 1997 event, observations of FAST and DMSP have shown that downward electron flux increased above the auroral oval after the shock arrival. Whether this increase was caused by the loss-cone instability or field-aligned currents is unknown at this time. But FAST detected that broadband wave activity increased by shock compression. The energy of the downward electrons had peaks at ~ 10 eV and 1 keV at FAST and 100 eV and 5 keV at DMSP.

Field-aligned current generation/enhancement is another shock-aurora mechanism suggested by the same authors as above. Field-aligned currents can be generated and coupled into the ionosphere when solar wind pressure disturbances impinge upon the magnetopause (Kivelson and Southwood, 1991). Sibeck (1990) has used a bulge-and trough-like turbulence to describe the magnetopause disturbance caused by a solar wind pressure pulse. Simultaneously, a double vortex is formed just at the earthward side of the magnetopause, based on Sibeck's model. This vortical flow may drive a guided shear wave which excites a dipolar field-aligned current, which in turn drives a vortical flow in the ionosphere (Kivelson and Southwood, 1991). This vortical flow is also called an ionospheric traveling convection vortex. Using the data from ground-based magnetometer arrays at high latitude, vortices often seem to occur in a bipolar signature or a single pulse (Friss-Christensent et al., 1988; Glassmeier et al., 1989; McHenry et al., 1989).

In this scenario, the ionospheric vortical flow will more likely occur away from local noon, on the flanks. A statistical study by Glassmeier et al., (1989) also found that 95% of ionospheric traveling convection vortices occurred within 05-11 LT. They call them a magnetospheric dawnside phenomenon. For the Nov 22, 1997 event, the Scandinavia magnetometers detected magnetic vortices on closed field lines just after the shock arrival at 0949:16 UT. The MLT region of the stations was 1204 (Andenes station) to 1300 (Kevo station) MLT. With the calculated shock normal at (-0.97, -0.145, 0.17) GSM coordinates, the tangential point of the shock at the magnetopause was ~ 1234 MLT. Thus, the magnetic fields with foot points at the

IMAGE stations were directly compressed by the shock at the tangential region. The model of a bulge-and trough-like turbulence at the magnetopause flanks (Figure 2. of Sibeck, 1990) can't explain the vortex formation in this event.

However, as shown in Figure 5, in the meridional plane that the tangential point was in, magnetopause distortions will also form on the magnetopause higher latitude regions (A and A' regions) when shocks compress the magnetopause and propagate anti-sunward. As shown by line 1, 2 and 3, the distortion is different at different L-shells and causes magnetic shearing between them. The magnetic shearing will lead to field-aligned currents into the ionosphere. It should be noted that magnetic reconnection will occur when the IMF B_z is southward, which is true for this Nov 22, 1997 event. This reconnection might be the cause of the different magnetic field changes between high and low latitude stations, as shown in Figure 4.

The generation of field-aligned currents by magnetic shears/field-line distortions can be estimated, following the work of Haerendel (1994). Using Ohm's law:

$$j_{//} = k\,\Phi_{//}\,, \qquad (1)$$

where $k^{-1} = Rw^2$, w is the width of current sheet, R is the mirror impedance equal to $m_e C_{BL}/e^2 n_{BL}$, and m_e, C_{BL}, e and n_{BL} are the electron mass, Alfvén speed in the boundary layer (BL), the electron charge and the plasma density in the BL. We can assume a field-aligned current focusing from the low latitude boundary layer (LLBL) to the ionosphere:

$$j_{//} = j_{//BL}\, B_{IO}/B_{BL}\,, \qquad (2)$$

where $j_{//BL}$ is the parallel current in the BL associated with the perturbation magnetic field $B_\perp$, while B_{IO} and B_{BL} are the field magnitudes of the ionosphere and BL. We have used the measured values of the BL (B_{BL} = 30 nT, n_{BL} = 1 cm^{-3}, C_{BL}= 600 km/s), the Russell and Elphic (1978) determination of the width of the BL (500 km), and B_{IO} = 0.5 Gauss. Assuming a perturbation field of $B_{\perp}$= 30 nT, a potential of ~ 2 kV was derived, which is a very reasonable value of electron energies for creating a discrete aurora.

This calculated result is also consistent with the observations of FAST and DMSP, the downward electron energy has a peak at 1-5 keV. So in this November 22, 1997 event, the shock-auroras should include at lease discrete auroras caused by these electrons. However, further confirmation is needed from ground-based imaging observations.

Acknowledgements: Portions of this research were performed at the Jet Propulsion Laboratory, California Institute of Technology, Pasadena, under contract with NASA. X.-Y. Zhou would like to thank J.K. Arballo for helping in the data processing and software support.

References

Arballo, J.K., C.M. Ho, G.S. Lakhina, B.T. Tsurutani, X.-Y. Zhou, Y. Kamide, J.-H. Shue, S.-I. Akasofu, R.P. Lepping, A.S. Sharma, C.C. Goodrich, K. Papadopoulos, and J.G. Lyon, Pseudobreakups during January 10, 1997, *International Conference on Substorms-4*, ed. Y. Kamide and S. Kokubun, pp. 315-318, Terra Sci., Tokyo, 1998.

Craven, J.D., L.A. Frank, C.T. Russell, E.E. Smith, and R.P. Lepping, Global auroral responses to magnetospheric compressions by shocks in the solar wind: Two case studies, in *Solar Wind-Magnetosphere Coupling*, ed. Y. Kamide and J.A. Slavin, pp. 367-380, Terra Scientific, Tokyo, 1986.

McHenry, M.A., C.R. Clauer, E. Friis-Christensen, and J.D. Kelly, Observations of ionospheric convection vortices: Signatures of momentum transfer, *Adv. Space Res., 8*, 315, 1989.

Murphree, J.S., R.D. Elphinstone, D. Hearn, and L.L. Cogger, Large-scale high-latitude dayside auroral emissions, *J. Geophys. Res., 95*, 2345, 1990.

Friis-Christensen, E., M.A. McHenry, C.R. Clauer, and S. Vennerstrom, Ionospheric traveling convection vortices observed near the polar cleft: A triggered response to sudden changes in the solar wind, *Geophys. Res. Lett., 15*, 253, 1988.

Glassmeier, K.-H., M. Honisch, and J. Untiedt, Ground-based and satellite observations of traveling magnetospheric convection twin vortices, *J. Geophys. Res., 94,* 2520, 1989.

Russell, C.T., and R.C. Elphic, Initial ISEE magnetometer results: Magnetopause observations, *Space Sci. Rev., 22,* 691, 1978.

Sitar, R.J., J.B. Baker, C.R. Clauer, A.J. Ridley, J.A. Cumnock, V.O. Papitaashvili, J. Spann, M.J. Brittnacher, and G.K. Parks, Multi-instrument analysis of the ionospheric signatures of a hot flow anomaly occurring on July 24, 1996, *J. Geophys. Res., 103*, 23357, 1998.

Sibeck, D.G., A model for the transient magnetospheric response to sudden solar wind dynamic pressure variations, *J. Geophys. Res.*, *95*, 3755, 1990.

Sibeck, D.G., N.L. Borodkova, S.J. Schwartz, C.J. Owen, R. Kessel, S. Kokubun, R.P. Lepping, R. Lin, K. Liou, H. Luhr, R.W. McEntire, C.-I. Meng, T. Mukai, Z. Nemecek, G. Parks, T.D. Phan, S.A. Romanov, J. Safrankova, J.-A. Sauvaud, H.J. Singer, S.I. Solovyev, A. Szabo, K. Takahashi, D.J. Williams, K. Yumoto, and G.N. Zastenker, Comprehensive study of the magnetospheric response to a hot flow anomaly, *J. Geophys. Res., 104,* 4577, 1999.

Southwood, D.J., and M.G. Kivelson, The magnetohydrodynamic response of the magnetospheric cavity to changes in solar wind pressure, *J. Geophys. Res.*, *95*, 2301, 1990.

Spann, J.F., M. Brittnacher, R. Elsen, G.A. Germany, and G.K. Parks, Initial response and complex polar cap structures of the aurora in response to the January 10, 1997 magnetic cloud, *Geophys. Res. Lett.*, *25*, 2577, 1998.

Torr, M.R., D.G. Torr, M. Zukic, R.B. Johnson, J. Ajello, P. Banks, K. Clark, K. Cole, C. Keffer, G. Parks, B. Tsurutani, and J. Spann, A far ultraviolet imager for the international solar-terrestrial physics mission, *Space Sci. Rev.*, *71*, 329, 1995.

Tsurutani, B.T., X-Y. Zhou, V.M. Vasyliunas, G. Haerendel, and J.K. Arballo, Interplanetary shocks, magnetopause boundary layers and dayside auroras, *Surv. in Geophys.*, in press, 2001a.

Tsurutani, B.T., X.-Y. Zhou, J.K. Arballo, W.D. Gonzalez, G.S. Lakhina, V. Vasyliunas, J.S. Pickett, T. Araki, H. Yang, G. Rostoker, T.J. Hughes, R.P. Lepping, and D. Berdichevsky, Auroral zone dayside precipitation during magnetic storm initial phases, *J. Atmos. Solar-Terr. Phys.*, *63*, 513, 2001b.

Zhou, X.-Y., and B.T. Tsurutani, Rapid intensification and propagation of the dayside aurora: Large scale interplanetary pressure pulses (fast shocks), *Geophys. Res. Lett.*, *26*, 1097, 1999.

Figure Captions

Figure 1. (A) The November 22, 1997 interplanetary shock event observed by the WIND spacecraft. (B) Corresponding auroral brightenings observed by POLAR UVI. A magnetic coordinate system is used, with magnetic local noon at the top and dawn at the right of the images.

Figure 2. FAST data from a southern dawnside auroral zone pass on November 22, 1997. From top to bottom: Panel 1 is the electric field component perpendicular to B that lies nearly along the spacecraft velocity vector, V_{sc}. Panel 2 is the magnetic deflection, positive east. Panel 3 is the total upgoing and downgoing electron energy flux. Panels 4 and 5 are electron energy and pitch angle spectrograms. (a) is prior to the shock arrival. (b) is after the arrival (Courtesy of C. Carlson).

Figure 3. The DMSP F14 plasma spectrogram from 0958 to 1022 UT (Courtesy of P. Anderson).

Figure 4. Magnetic perturbations caused by the interplanetary shock observed on November 22, 1997, by IMAGE ground magnetometers. (a) is a map of IMAGE stations. (b) is the X-component stack plot (Courtesy of Finnish-German-Norwegian-Polish-Russian-Swedish project).

Figure 5. A schematic for magnetopause distortions in the meridional plane. The shaded area is the dayside magnetopause.

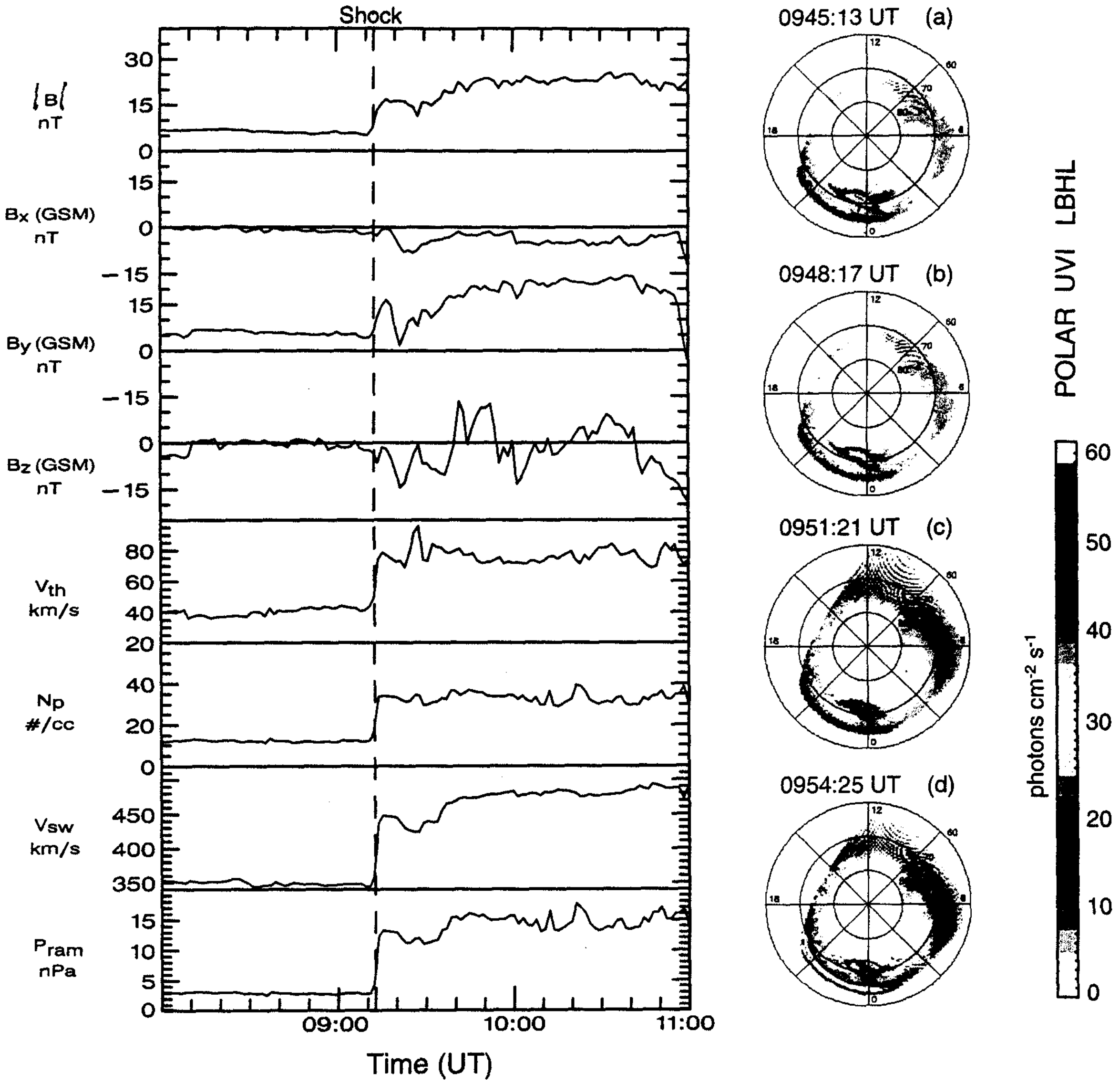

Shock
|B|
nT
Bx (GSM)
nT
By (GSM)
nT
Bz (GSM)
nT
Vth
km/s
Np
#/cc
Vsw
km/s
Pram
nPa
09:00
10:00
11:00
Time (UT)
0945:13 UT (a)
0948:17 UT (b)
0951:21 UT (c)
0954:25 UT (d)
POLAR UVI LBHL
photons cm-2 s-1

(A)

(B)

Figure 1

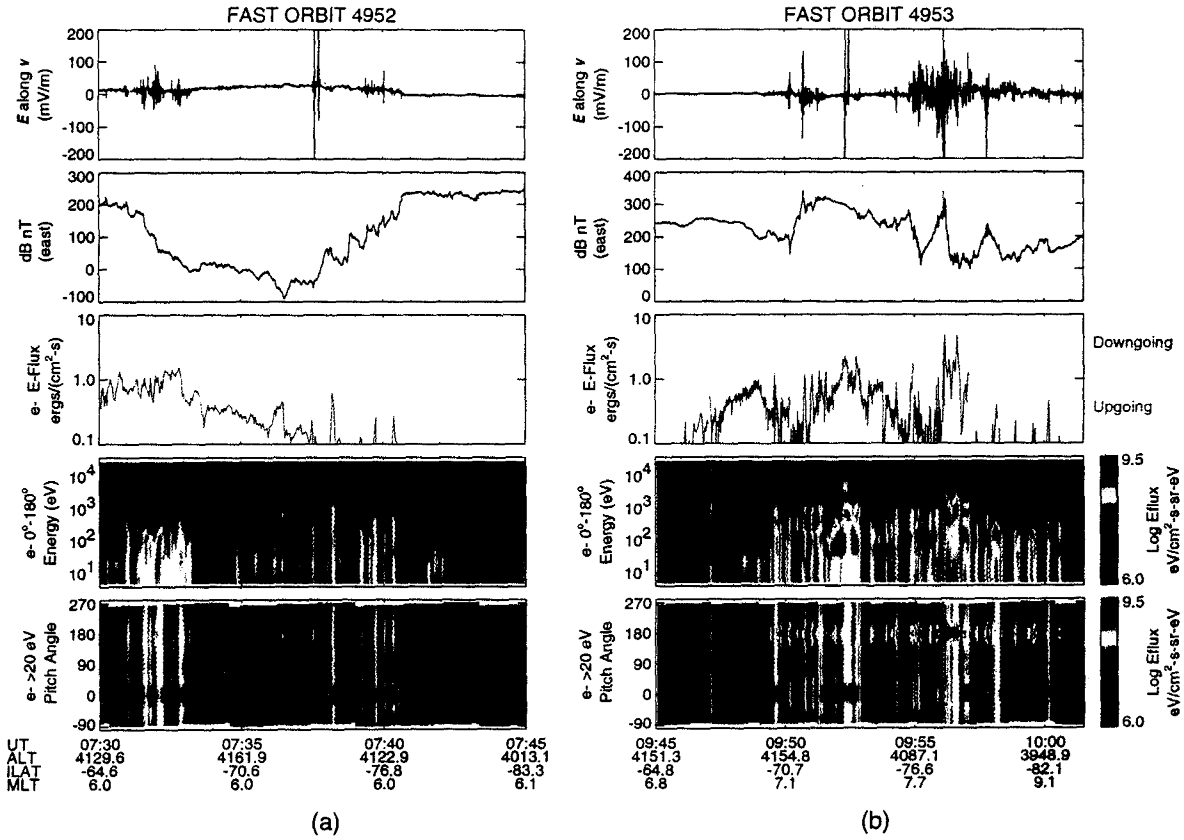

FAST ORBIT 4952
FAST ORBIT 4953
E along v (mV/m)
dB nT (east)
e- E-Flux ergs/(cm²-s)
e- 0°-180° Energy (eV)
e- >20 eV Pitch Angle
Downgoing
Upgoing
Log Eflux eV/cm²-s-sr-eV
UT 07:30 07:35 07:40 07:45
ALT 4129.6 4161.9 4122.9 4013.1
ILAT -64.6 -70.6 -76.8 -83.3
MLT 6.0 6.0 6.0 6.1
UT 09:45 09:50 09:55 10:00
ALT 4151.3 4154.8 4087.1 3948.9
ILAT -64.8 -70.7 -76.6 -82.1
MLT 6.8 7.1 7.7 9.1
(a)
(b)

Figure 2

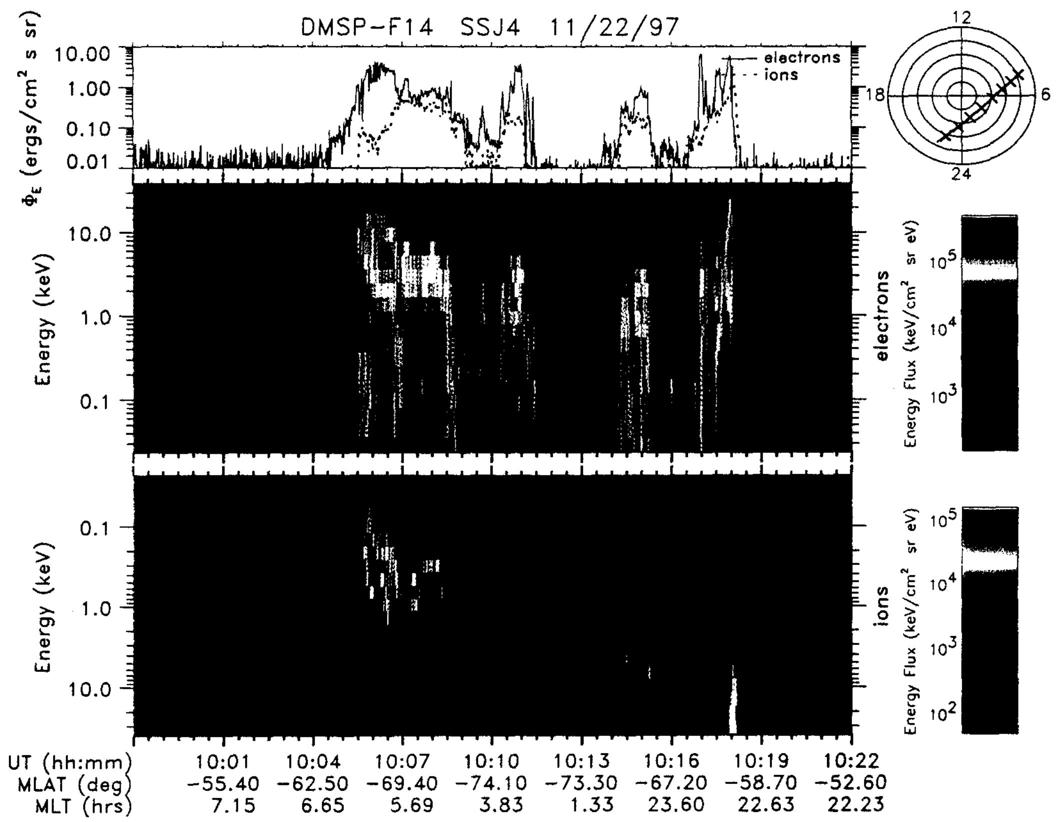

DMSP-F14 SSJ4 11/22/97
Φ_E (ergs/cm² s sr)
10.00
1.00
0.10
0.01
electrons
ions
12
18
6
24
Energy (keV)
10.0
1.0
0.1
electrons
Energy Flux (keV/cm² sr eV)
10⁵
10⁴
10³
Energy (keV)
0.1
1.0
10.0
ions
Energy Flux (keV/cm² sr eV)
10⁵
10⁴
10³
10²
UT (hh:mm) 10:01 10:04 10:07 10:10 10:13 10:16 10:19 10:22
MLAT (deg) -55.40 -62.50 -69.40 -74.10 -73.30 -67.20 -58.70 -52.60
MLT (hrs) 7.15 6.65 5.69 3.83 1.33 23.60 22.63 22.23

Figure 3

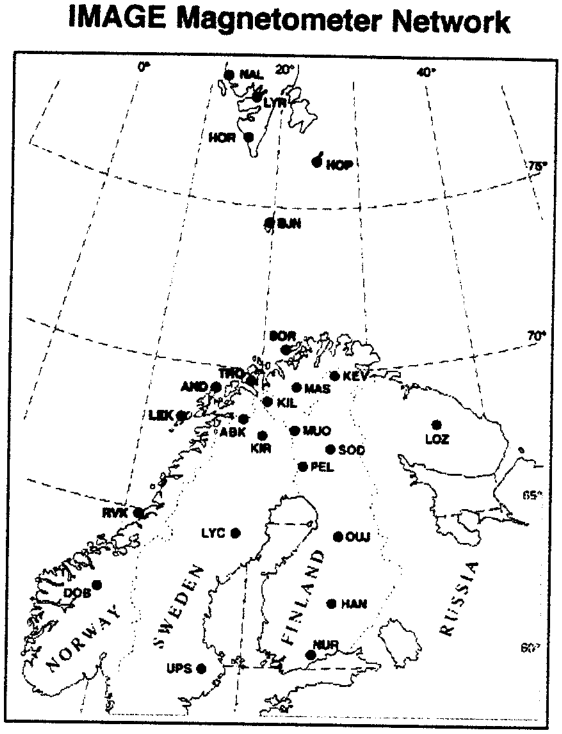
IMAGE Magnetometer Network
0°
20°
40°
75°
70°
65°
60°
NAL
LYR
HOR
HOP
BJN
SOR
TRO
AND
KEV
MAS
KIL
LEK
ABK
KIR
MUO
SOD
PEL
LOZ
RVK
LYC
OUJ
DOB
HAN
NUR
UPS
NORWAY
SWEDEN
FINLAND
RUSSIA

(a)

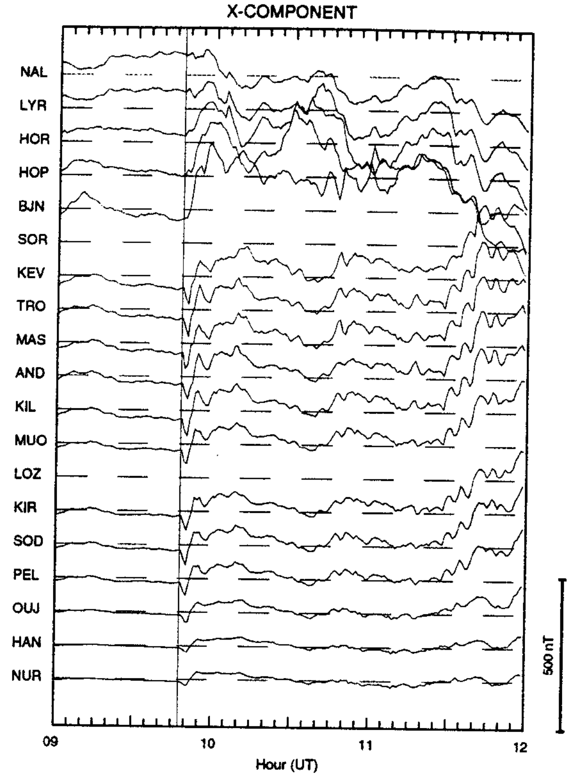
X-COMPONENT
NAL
LYR
HOR
HOP
BJN
SOR
KEV
TRO
MAS
AND
KIL
MUO
LOZ
KIR
SOD
PEL
OUJ
HAN
NUR
09
10
11
12
Hour (UT)
500 nT

(b)

Figure 4

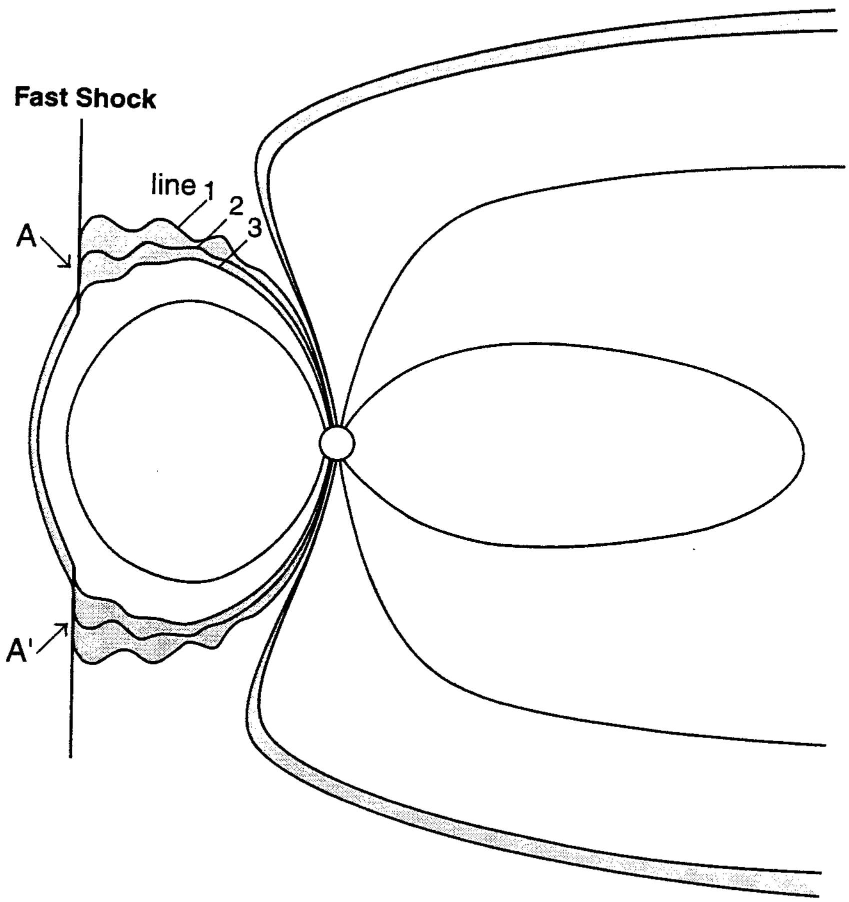

Figure 5